# Both sides now: Optimal bifaciality with silicon heterojunction solar cells

Adrien Danel, Julien Eymard, Vincent Barth, Mathieu Tomassini, Eric Gerritsen, Armand Bettinelli & Charles Roux, CEA, LITEN, Department of Solar Technologies, INES, Grenoble, France

## Abstract

Silicon heterojunction (SHJ) solar cells are by nature bifacial, and their back-to-front ratio (bifaciality) can be easily tuned by means of the pattern of the metal grid on the front and back sides. This paper discusses, at both the cell and the module level, the balance between the advantages and drawbacks of increasing the cell bifaciality from a typical value of 90% towards 100%, or decreasing it towards that of monofacial cells (0%). For outdoor operation with extra light hitting the back side, the effective performance of bifacial systems was estimated with regard to the trade-off between cell efficiency and bifaciality. This work presents how very high bifaciality comes at a cost of lower (front-side) conversion efficiency, and discusses how the amount of silver paste per cell, a main contributor of cell cost, is strongly related to cell bifaciality and efficiency. The use of a symmetric grid pattern is one easy way of obtaining highly bifacial cells, but at the expense of high resistivity in the case of metal grids using a typical front-side pattern. On the other hand, a rear-side pattern used on the front and back sides can lead to a situation where there is excessive shading. Furthermore, the efficiency of a rear-emitter cell decreases at very high bifaciality with the use of thinner amorphous layers on the back side, necessary for symmetrizing the light absorbance of the cell. Thus, an optimum can be found for a given system design operating with a given irradiance at the back side. Similarly, for a given type of cell, systems can be specifically designed to optimize the benefits of the given cell bifaciality. The output of tilted modules is maximum when a large proportion of light comes from the back side, with cell bifaciality ranging from 85% to 95%. The use of an optimal metal grid can offer a relative gain in energy production, as high as 3%, and typically corresponds to a front-side metal grid pitch from 1.2 to 2mm and a back-side pitch from 0.6 to 0.9mm. When specific applications are considered where a symmetrical print is preferred for building-integrated or vertically oriented systems, the optimal grid pitch is around 1.5mm. For monofacial systems, the use of bifacial cells is beneficial, thanks to the internal reflection in glass-backsheet modules and because of the cost saving for additional rear-metallization.

*Reproduced, with permission, from Willocket et al. [8].*

**Figure 1. Pilot agri-PV in an orchard at Bierbeek, Belgium, illustrating the benefit of bifacial cells for high-transparency modules placed at a high elevation.**

## Bifacial is blooming

True bifacial PV systems are today entering real deployment with a 14-fold increase expected over the next five years, as forecast by ITRPV [1]. It is no longer a niche technology reserved for cells with the highest efficiencies, but a 'giant leap for kWh cost reduction' [2] applied to the main current and future cell technologies: PERC (passivated emitter rear cell), PERT (passivated emitter rear totally diffused), TOPCon (tunnel oxide passivated contact), SHJ (silicon heterojunction) and even IBC (interdigitated back contact). Accordingly, an estimation of the bifacial benefit of individual installations has recently been intensively studied [3], with simulations [4] and experimental field data [5], including the LCOE (levelized cost of electricity) [6,7]. These studies, based on a given type of cell and module, are very useful to PV installation companies for selecting the most relevant technologies and for optimizing their designs when considering operational conditions for particular projects, as illustrated in Fig. 1 [8]. However, ahead of this, the possibility of adapting the bifaciality of cells has so far been poorly taken into consideration.

With their symmetrical structure, SHJ solar cells made of very thin hydrogenated amorphous silicon layers (a-Si:H), transparent conductive oxides (TCO), and metallization grids deposited on both sides of the wafers are by nature bifacial [9]. This paper is a continuation of a study [10] in which the bifaciality of busbar and busbar-less SHJ cells ($BF_{cell}$) was varied using different metallization grid patterns; the subsequent impact on cell efficiency was investigated in order to estimate the system output versus the amount of light at the back side. Here, the way the differences in thin films deposited on the front and rear sides affect the bifaciality will also be presented, and the possibilities of approaching a cell bifaciality of 100% will be discussed.

## Experimental details and methodology

The cell manufacturing was performed on the CEA SHJ pilot line [11] located at INES, the French National Solar Energy Institute, using a rear-emitter double-side-contacted (screen printing with low-temperature Ag paste) configuration on full-size commercial n-type Cz wafers (M2 size, 244.3cm², from Longi). The bifaciality factor of each *I–V* parameter is the back-to-front ratio measured under standard test conditions (STC). $BF_{cell}$ is the lowest value coefficient, usually the power one.

The cell bifaciality was first varied using different finger pitches on busbar-less (BB-less) and busbar (BB) grid patterns. The configurations in this study range from a very dense grid on the back side for low bifaciality, to identical-spaced grids on the front side (FS) and the back side (BS) in order to achieve high bifaciality and symmetrical-looking cells. In practice, the finger pitch varied from 0.2 to 2.1mm. All *I–V* measurements were performed over the total area under AM1.5G STC using an *I–V* tester without back-side reflection, calibrated against sister cells certified by the FhG ISE CalLab and ISFH CalTeC. Each bifaciality experiment with a given design (BB-less or BB) was carried out on cells from the same production run using the CEA-INES baseline process flow. Sets of cells were randomly selected for each screen-printing batch, and labelled according to the FS and BS grid pitch (mm), as illustrated in Fig. 2 with an example of data for a BB design.

Next, similarly to the IEC 60904-1-2 standardization work [3,5], BB-less and BB cell efficiency as a function of $BF_{cell}$ (see Fig. 3) data were used to calculate a figure of merit for bifacial systems. Equation 1 represents tilted modules, where *BIFI* is the back-side irradiance relative to the front-side irradiance, in per cent. As an example, $BIFI_{20}$ corresponds to an equivalent of 200W/m² on the back side when the front side is illuminated by 1000W/m². Equation 2 represents vertical east–west-oriented modules (V-EW), for which direct sunlight shines for half the time on the front side and for

**"With their symmetrical structure, SHJ solar cells made of very thin a-Si:H layers, TCO and metallization grids deposited on both sides of the wafers are by nature bifacial."**

half the time on the back side, with the same irradiance on the rear of the panel, i.e. the same BIFI factor. In other words, first (i.e. in the morning) the back side is the 'true' rear side of the module, then (in the afternoon) the back side becomes the side of the module receiving mostly direct light. Possible differences between the average *BIFI* during the morning and the afternoon are not considered here.

$$\eta_{system} = \eta_{cell} \times CTM \times (1 + BF_{module} \times BIFI) \quad (1)$$

$$\eta_{system} = \eta_{cell} \times CTM \times [0.5(1 + BF_{module} \times BIFI) + 0.5\,(BF_{module} + BIFI)] \quad (2)$$

where,

$\eta_{system}$ is the system output (figure of merit),
$\eta_{cell}$ is the front-side STC power conversion efficiency,
*CTM* is the cell-to-module loss ratio,
$BF_{module}$ is the module bifaciality factor estimated from practical $BF_{cell}$,
*BIFI* is the average of the overall light input at the back side, levelled over one year. (Note that, strictly speaking, the back side of a V-EW system alternates for half the day between the true back side and the front side of the system.)

In this work, the intention is not to define bifaciality factors for particular cases. From the literature [3–6] and CEA's own field data for SHJ systems [7,12], the range of practical *BIFI* one can deal with worldwide is simply extracted: the $\eta_{system}$ as a function of $BF_{cell}$ for values of *BIFI* ranging from 0 to 40% was therefore studied in order to determine the optimal SHJ cell bifaciality factor for a given module technology operating at a specific bifaciality factor. This simple approach was taken, whatever the actual parameters determining the bifaciality factor, such as system design (module tilt and elevation above ground, number of modules and rows, spacing, etc.), system orientation, geographical location, typical meteorological year, ground albedo, surroundings, and so on, and whatever the temporary *BIFI* variations for different weather conditions [13].

The $BF_{module}$ coefficients are the experimental $BF_{cell}$ data corrected for the effective grid shading: 95% in air and around 72% in a module [14]; this important factor was verified in practice, as reported in Danel et al. [10]. Indeed, the effective bifaciality of cells in a module is always higher than that of bare cells in air, with the difference increasing as $BF_{cell}$ decreases.

Despite this approach possibly not strictly representing all applications (for example, new systems with very low cell coverage specifically designed for agriculture, where bifaciality is must, as illustrated in Fig. 1 [8]), the trend of $\eta_{system}$ as a function of $BF_{cell}$ allows the determination of an optimal cell design for a given system project.

In addition to the practical data, a two-diode model was developed in-house and used to simulate efficiency and power response at the cell and module levels for various bifaciality and *BIFI* conditions. Key electrical and optical parameters are assumed to fully represent module and cell design, including the material properties and heterojunction specificities. The series resistance ($R_s$) of the metallization is modelled from the resistivity of: 1) low-temperature silver paste; 2) electrically conductive adhesive; and 3) ribbons. This modelling takes into consideration the effective shape of each of the three resistivity elements.

The bulk resistance of the crystalline silicon substrate and the TCO layers is taken into account, so that changes in lateral transport of charges can be considered when the pattern of the metal grids varies [8]. This simulation also includes the losses

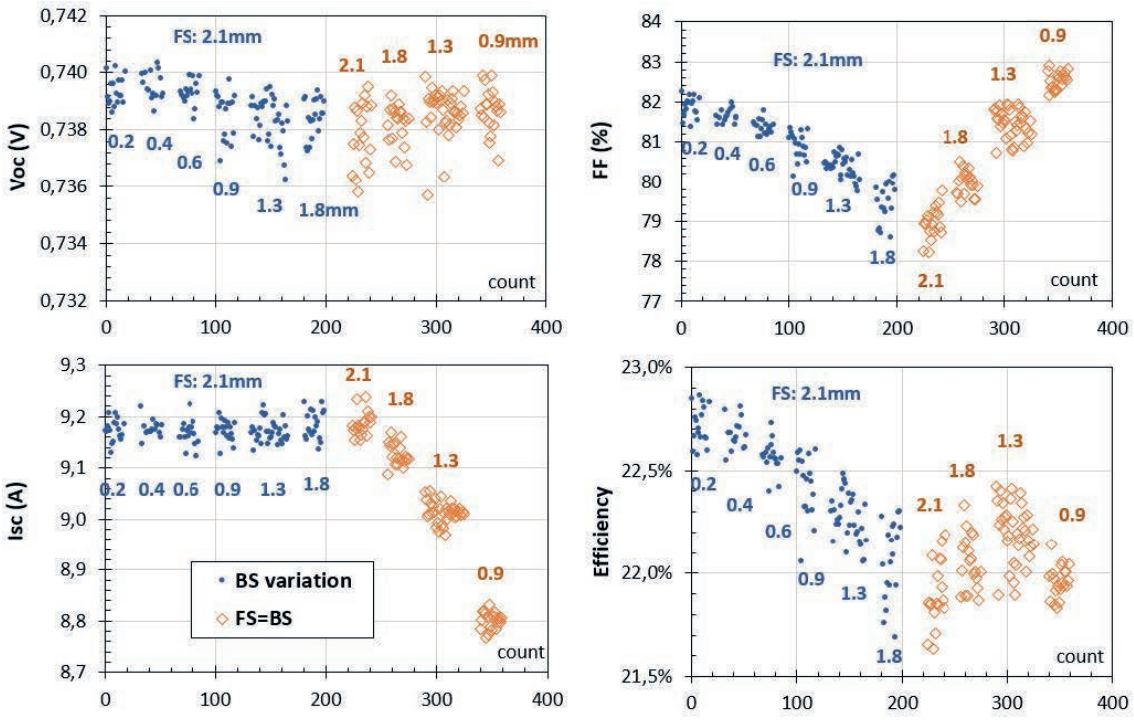


Adapted from Danel et al. [10].

**Figure 2. Bifaciality experiments on BB cells, where the back- and front-side metal grid pitch (noted in mm) was varied while keeping the same screen parameters (mesh, emulsion, opening, etc.). The cell-to-cell main *I*–*V* parameters are plotted using blue dots for asymmetric prints and orange diamonds for symmetric prints.**

in performance of cells after being cut in order to allow for modules with half-cells or third-cells. The effective shapes of the grids (number and shape of fingers and busbars), and the reflectivity, absorbance and transmittance of materials (cells, glasses, encapsulants, metal grids and ribbons), are measured and considered for assessing the optical behaviour of the modules [15,16].

## Cell efficiency versus bifaciality

The bifaciality factors of each *I–V* parameter were measured for the cells in Fig. 1, as well as for two other similar experiments in which the pitch of fingers in the BS grid were varied while keeping the same FS grid. The quantity $BF_{cell}$ is the power bifaciality, mainly driven by the short-circuit current ($I_{sc}$) bifaciality.

The average cell efficiency of each batch is plotted against $BF_{cell}$ in Fig. 3. The SHJ cell efficiency shows a steady decay from a monofacial to a highly bifacial design, with a significant drop in the highest cell bifaciality values being obtained when identical-spaced grids FS and BS are used (2.1mm and 2.1mm in this study for the splits of cells having an indium tin oxide (ITO) at the back side). For the BB-less and ITO BS experiment, a couple of reference cells (pitch 2.1mm FS and 0.6mm BS) received an additional plain metallization rear side by silver physical vapour deposition (PVD) to produce monofacial cells. In Fig. 3 and Table 1, this is the batch of cells with a bifaciality of 3.4% and a +0.16%$_{abs}$ efficiency compared with the reference batch.

The efficiency decay is similar for the BB and BB-less cell designs and is mainly related to the decrease in fill factor (*FF*) and increase in $R_s$, due primarily to the resistive contribution of the BS grid (as can be seen in Fig. 1). The test with $In_2O_3$-based TCO by PVD [17,18] at the back side illustrates how the lateral conduction of the TCO can also be an important limitation when increasing the pitch. Indeed, the very good material properties for charge collection on the p contact with a high transparency are counteracted by the limited lateral conduction. For this test, the good electrical properties of this material were intentionally degraded to boost the optical properties. Thus, if $In_2O_3$-based TCO can perform well with a dense grid BS, as well as offering significant improvement in FS cell efficiency, its integration in very high bifaciality cells is more delicate than when ITO is used.

It is worth noting that a bifaciality factor <100% is obtained for a symmetrical print as a result of the rear-emitter cell optimization for a maximum front-side efficiency at STC. This is achieved with different hydrogenated amorphous silicon stacks (a-Si:H) and TCO thicknesses and electro-optical properties on the FS and BS in order to ensure a high minority-carrier lateral conduction [19] in a good balance with transparency.

Conversely, a monofacial design offers a bonus

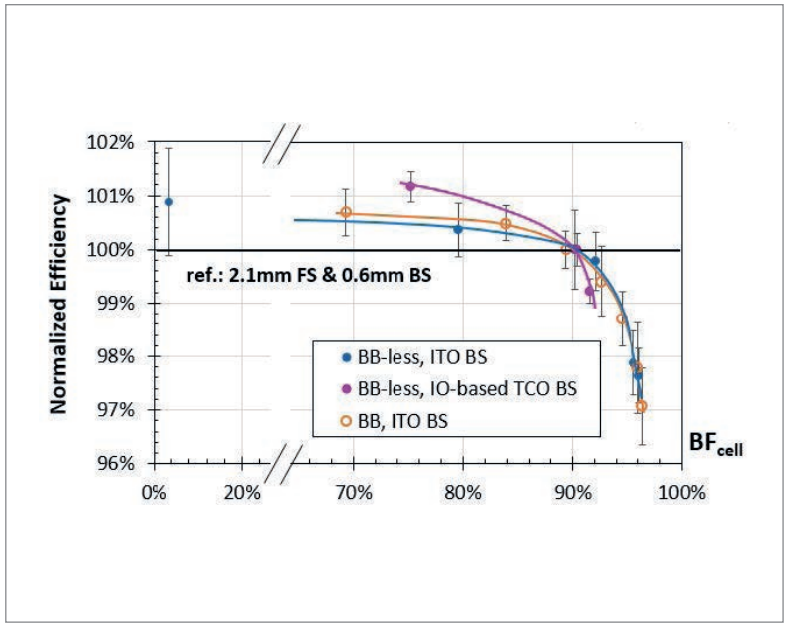


**Figure 3. BB and BB-less normalized cell efficiency as a function of cell bifaciality. The dots/circles represent the average, and the error bars the standard deviation of each cell batch. The reference is the 2.1mm FS and 0.6mm BS print. Two different TCOs are considered here. The solid lines have been added as a visual guide.**

for the FS *I–V* data of SHJ cells, but the +0.16%$_{abs}$ seen in practice requires an extra process step with associated costs. Furthermore, the use of monofacial cells for monofacial applications is not useful. In previous work carried out by CEA [10], a similar power output was obtained for glass-backsheet modules with white encapsulant and bifacial cells thanks to a better CTM coefficient using the reference print (90% $BF_{cell}$) compared with true monofacial cells. This result occurred by virtue of an 'embedded' bifaciality, with a good reflection onto the encapsulant and backsheet of both the incident light entering the module in between the cells and the near-infrared light passing through the cells.

Table 1 summarizes typical *I–V* values for CEA's SHJ cells with ITO on both sides and with processes optimized with the reference print. This illustrates the latitude one may have in optimizing cells for a given system application, taking into account efficiency, bifaciality and costs (amount of silver paste).

## Towards 100% bifaciality: virtues and vices

With symmetric ITO and prints on the FS and BS, a $BF_{cell}$ of around 95% is obtained. This 'intrinsic' cell bifaciality, the highest value in Fig. 3, is related to the asymmetry between the a-Si:H layers, with a thicker and less transparent intrinsic (i) and p-doped stack at the BS, and an i and n-doped stack at the FS. As studied in Danel et al. [10] and shown in Fig. 4, $BF_{cell}$ can be pushed above 98% using a very thin i and p a-Si:H stack. Layers that are too thin, however, can cause *FF* or $V_{oc}$ degradation, as plotted in Fig. 4(a). Starting from the plasma-enhanced chemical vapour deposition (PECVD) recipes normalized to 1 in Fig. 4 (blue arrows), an analysis was performed to find a good

| Metal | $\eta$ [%] | $V_{oc}$ [mV] | $J_{sc}$ [mA/cm$^2$] | *FF* [%] | Bifaciality [%] | Ag paste [mg] |
|---|---|---|---|---|---|---|
| Reference: 2.1/0.6mm | 22.70 | 737.4 | 38.33 | 80.26 | 90.2 | 117 |
| Monofacial | 22.86 | 738.2 | 38.47 | 80.46 | 3.4 | 117 + PVD Ag |
| 2.1/0.3mm | 22.74 | 737.6 | 38.31 | 80.46 | 79.6 | 212 |
| 2.1/0.9mm | 22.57 | 738.2 | 38.32 | 79.78 | 92.1 | 86 |
| Symmetric: 2.1/2.1mm | 22.13 | 737.7 | 38.30 | 78.32 | 96.1 | 44 |
| Optimized: 1.5/1.5mm | 22.40 | 737.2 | 38.39 | 79.10 | 96.1 | 56 |

**Table 1. Main *I–V* parameters of SHJ cells having various metallization patterns.**

"A bifaciality factor <100% is obtained for a symmetrical print as a result of the rear-emitter cell optimization for a maximum front-side efficiency at STC."

balance between the i and p layer thicknesses and tune the electrical properties. A 17%-thinner back-side stack was developed and ensures a 95–96% intrinsic bifaciality, without affecting FS cell efficiency (0.83 normalized point and the grey arrow in Fig. 4).

If $BF_{cell}$ >98% can be easily achieved by experimenting with a BS pitch larger than the FS pitch, or by using a thicker a-Si:H stack at the FS, this will be to the detriment of cell efficiency. Therefore, for very high bifaciality cells dedicated to applications, such as planar connections [16,20,21] or V-EW systems, where similar electrical performance is preferred in order to avoid electrical mismatch, the case of a symmetric print was considered and the pitch of the fingers varied.

As shown in the plots in Fig. 5, the use of a dense grid (typically a BS design) leads to an $I_{sc}$-limited cell efficiency, while the use of a large pitch (FS design) results in an *FF*-limited situation, mainly related to grid $R_s$ and lateral conduction in the TCO limitation on the rear side. Specific to CEA's printing process, an optimal pitch of about 1.5mm balances the $I_{sc}$ and *FF* limitation scenarios. It is worth noting

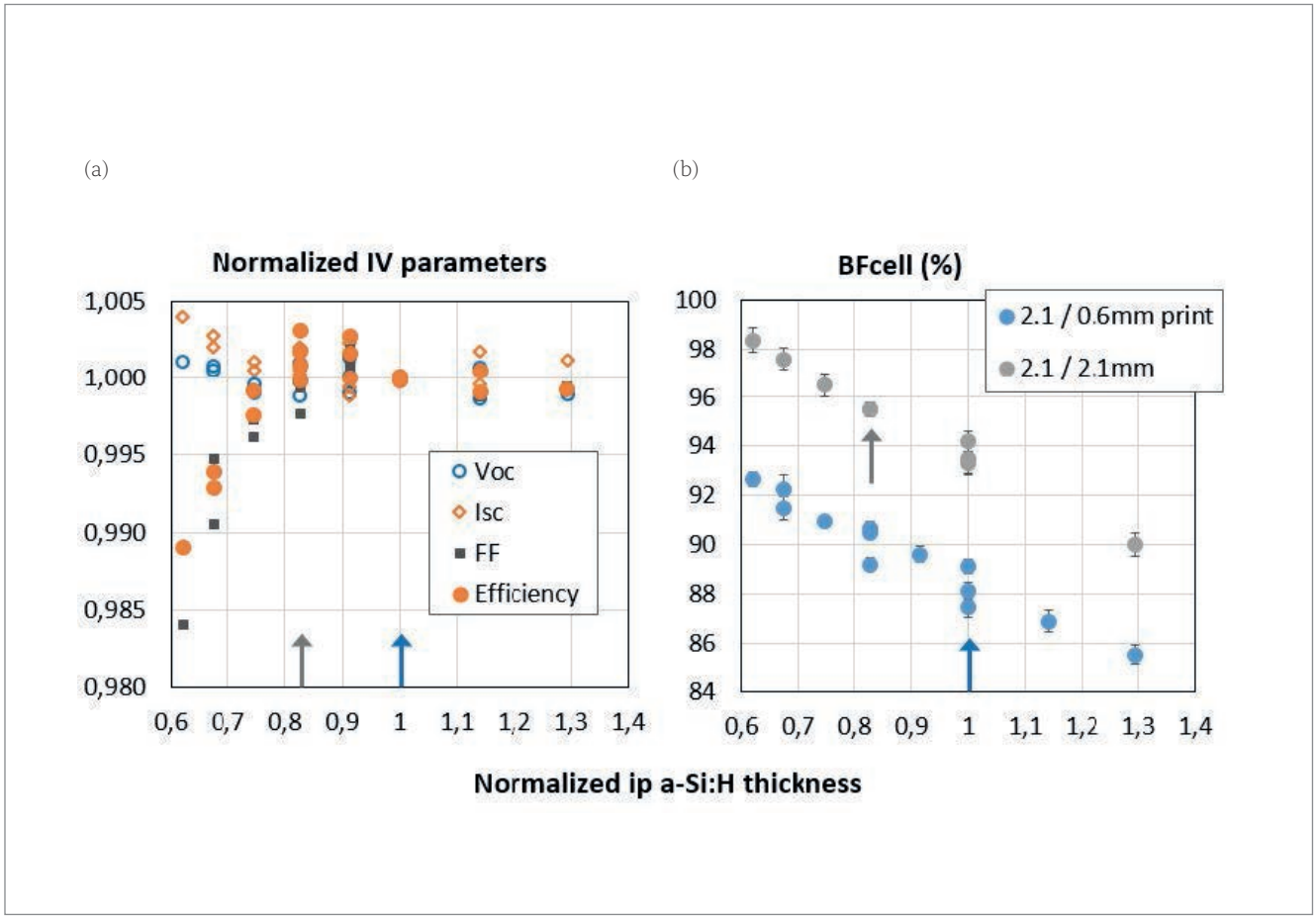


**Figure 4. i and p a-Si:H stack optimization to enhance cell bifaciality: (a) *I–V* data normalized to 1 for CEA's pilot line reference recipes; (b) corresponding cell bifacialities. Each point is the average of a multiple cell batch, and the error bars on graph (b) represent standard deviations.**

that all points in Fig. 5 have a bifaciality of about 95%, driven by the a-Si:H stacks asymmetry, as mentioned in the discussion of Fig. 4.

### Estimation of system output

The experimental cell data in Fig. 3 are used in the proposed figure of merit (Equations 1 and 2) to estimate the system energy output as a function of cell bifaciality, with the following assumptions:

1. A constant *CTM* of 0.98 (2% loss) for glass–glass industrial SHJ modules [22], independent of the value of $BF_{cell}$ (a hypothesis validated by experimental data from two mini-modules).

2. A bifaciality factor ranging from 0 to 40% in order to cover any practical system design and operating conditions.

3. A constant cell efficiency (STC value), whatever the value of the bifaciality factor. This simple hypothesis disregards possible average efficiency changes with different module temperatures in the morning and the afternoon, or with variations in *BIFI*. It might also not be valid for a precise estimation of system equivalent efficiency, since when the *BIFI* increases, the current increases by a factor $(1 + BIFI \times BF_{module})$, and accordingly the resistive losses might become important. However, thanks to the module simulation taking this into account, and with the aim of determining the optimal $BF_{cell}$ for a given bifaciality factor, the assumption can be considered to be valid.

Fig. 6 shows the estimation of system output, i.e. the equivalent efficiency of (a) tilted and (b) V-EW systems for various *BIFI*, for cells with ITO FS and BS and an 'intrinsic' bifaciality of about 96%. The arrows on the charts highlight the estimation of the optimal cell bifaciality for a given bifaciality factor. For the tilted module situation (Fig. 6(a)), the higher the *BIFI*, the higher the cell bifaciality. This is accompanied by a fairly strong dynamic for low *BIFI*: the optimal $BF_{cell}$ moves quickly from about 80% for $BIFI_5$ to 91% for $BIFI_{20}$. Then, interestingly, from a practical point of view, at higher *BIFI* the optimal $BF_{cell}$ increases more slowly and tends to saturate at about 92%. This typically corresponds to prints with a FS pitch of 2.1mm and a BS pitch between 0.6 and 0.9mm.

Compared with the tilted system in Fig. 6(a), the optimal $BF_{cell}$ for V-EW systems (Fig. 6(b)), is higher, at 93%, and almost constant, regardless of the value of *BIFI*. A symmetrical print offering

the highest cell bifaciality and nice aesthetics for vertical modules is not the best option for system output in this example with a 2.1mm pitch. However, as reported in Danel et al. [10] and illustrated in Fig. 5, with an intermediate pitch of around 1.5mm to optimize the FS cell efficiency, a very good equivalent efficiency for V-EW modules can be obtained with a symmetrical print.

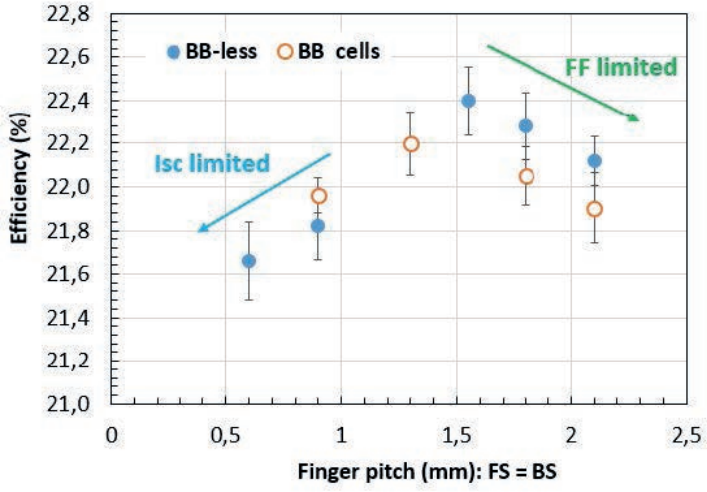


**Figure 5. Conversion efficiency of symmetrical cells.**

## Simulation of optimal bifaciality

To see more precisely how optimal cell bifaciality varies with *BIFI*, the data in Fig. 6(a) were normalized, as shown in Fig. 7(a), to find out the maximum equivalent efficiency for each *BIFI* value. The optimal cell bifaciality is plotted against *BIFI* in Fig. 7(b), which can then be used to select the best print design during cell manufacturing in order to optimize system output.

It is worth noting that the optimal $BF_{cell}$ becomes almost constant for high *BIFI* (92% in this example), while the relative loss rapidly increases for high *BIFI* when using a non-optimal cell bifaciality. The opposite is true at low bifaciality factors. As an example, for $BIFI_5$ the optimal $BF_{cell}$ is 82%, which is very different from the 92% at $BIFI_{40}$. However, if non-optimal cells are used, the relative loss is moderate for low *BIFI* applications, but significant at high *BIFI*. Given this, the best choice for mass production with a single design (or only a few designs) clearly leans towards high bifaciality, or, more precisely, the optimal value for high *BIFI*. Furthermore, this point goes hand in hand with cost reduction, with less silver paste being used on the back-side grid, as reported in Table 1.

In addition to the cell experiments, the module

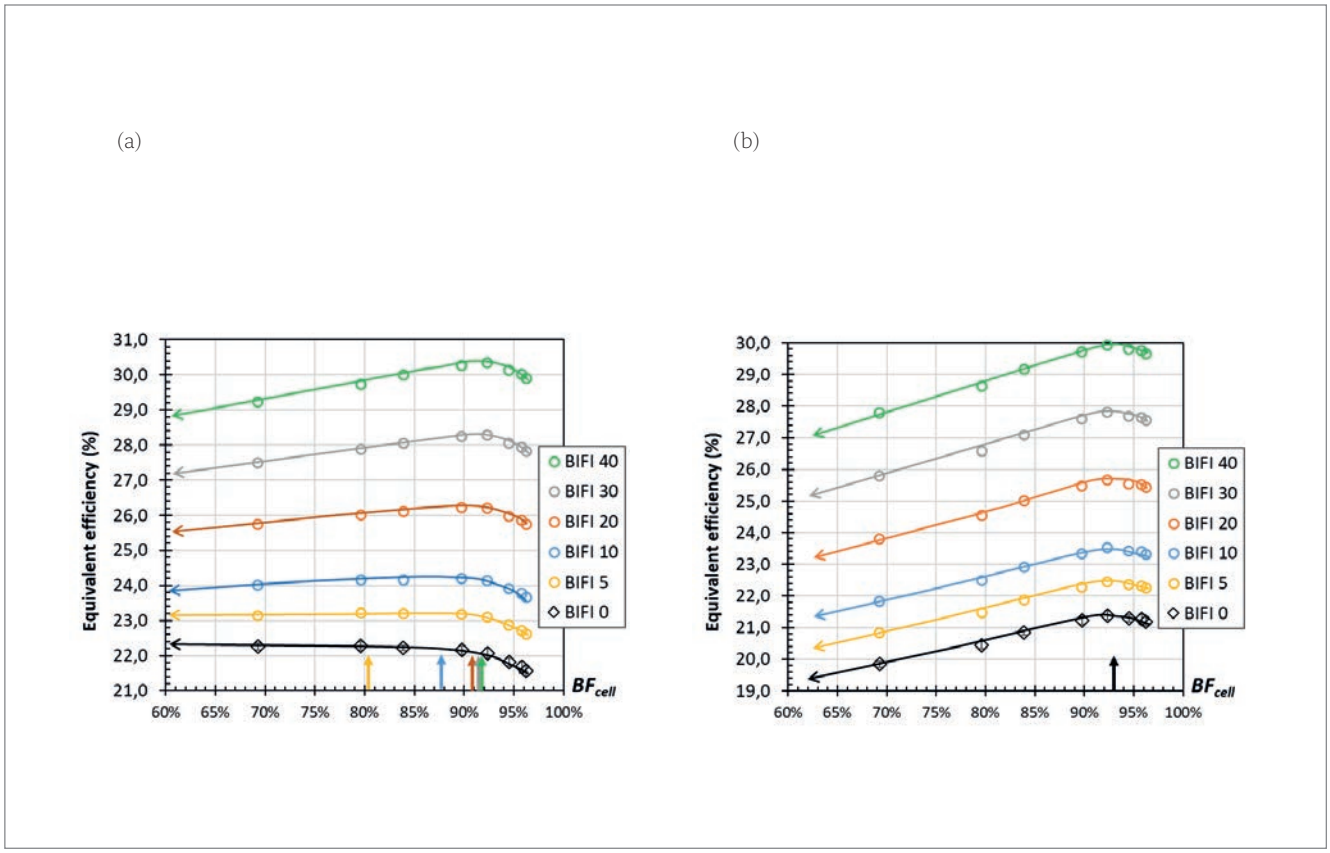


**Figure 6. System output variation as a function of cell bifaciality ($BF_{cell}$) for different percentage of back-side irradiance relative to the front-side irradiance (*BIFI*): (a) tilted system (Equation 1); (b) V-EW system (Equation 2). The solid lines have been added as a visual guide. The arrows indicate the optimal cell bifaciality for each *BIFI*.**

simulation developed in-house was applied to some practical situations. Fig. 8 summarizes the main outputs for 144 half-cell modules incorporating six-busbar M2 cells. For applications without light striking the back side of the cell (*BIFI* = 0), disregarding the silver paste cost issue, the higher the FS cell efficiency, the better the nominal power at STC. As shown in Fig. 8, the optimal grid pattern at $BIFI_0$ is 1.5mm FS and 0.1mm BS, giving 439.5Wp and a module bifaciality of 68.6%. With 300W/m² of light shining on the back side of the module ($BIFI_{30}$), the best cell design is a 1.2mm grid FS and 0.7mm BS. This corresponds to a 92.1% bifacial module delivering 554.5Wp. This design, with a fairly dense grid on the front side, ensures a situation favourable to *FF*. The current remains at a good value thanks to: 1) the 45µm-width fingers considered here; 2) the cell grid shading being lower inside the module; and 3) the significant contribution from the back with a $BIFI_{30}$ factor.

If the 0.1mm pitch for the BS grid is not used when systems with light on the back side are considered, the difference between the best and the worst grid patterns, for both $BIFI_{10}$ and $BIFI_{30}$, corresponds to around a 3% relative difference to the module Wp at STC multiplied by (1 + *BIFI*). As seen on the plot in Fig. 8, at $BIFI_{30}$ this corresponds to 554Wp using a 1.2mm FS/0.7mm BS pattern, and to 538Wp with 2.4/1.3mm. For $BIFI_{10}$, the best output is 477Wp, obtained with 1.5/0.4mm or 1.2/0.4mm grids,

"The best choice for mass production with a single design (or only a few designs) clearly leans towards high bifaciality."

and drops to 464Wp with 2.4/1.3mm.

## Conclusion and perspectives

SHJ cells are inherently bifacial and their bifaciality factor ($BF_{cell}$) can be easily tuned, from 0% for a monofacial cell to typically 90% for bifacial cells, and even 100%, but at the expense of front-side efficiency.

For outdoor operation with extra light at the back side (BIFI factor), the effective performance of bifacial systems increases with cell bifaciality ($BF_{cell}$), provided the efficiency decay remains limited. Up to a cell bifaciality of about 90% considered in this work, the precise value depends mainly on the asymmetry of the a-Si:H stacks. The rate of decrease is more pronounced for very high bifaciality because of the drop in front-side (FS) cell efficiency with an increase in $R_s$ (related to both the longer lateral conduction in TCO and the increase in resistivity of the back-side (BS) metal grid), or to the shading of the FS grid.

Thus, an optimal $BF_{cell}$ can be found for a given ratio of back-side to front-side irradiance. From practical cell and module data, when the system bifaciality is varied by means of the screen-printed grid asymmetry, the system output is maximum

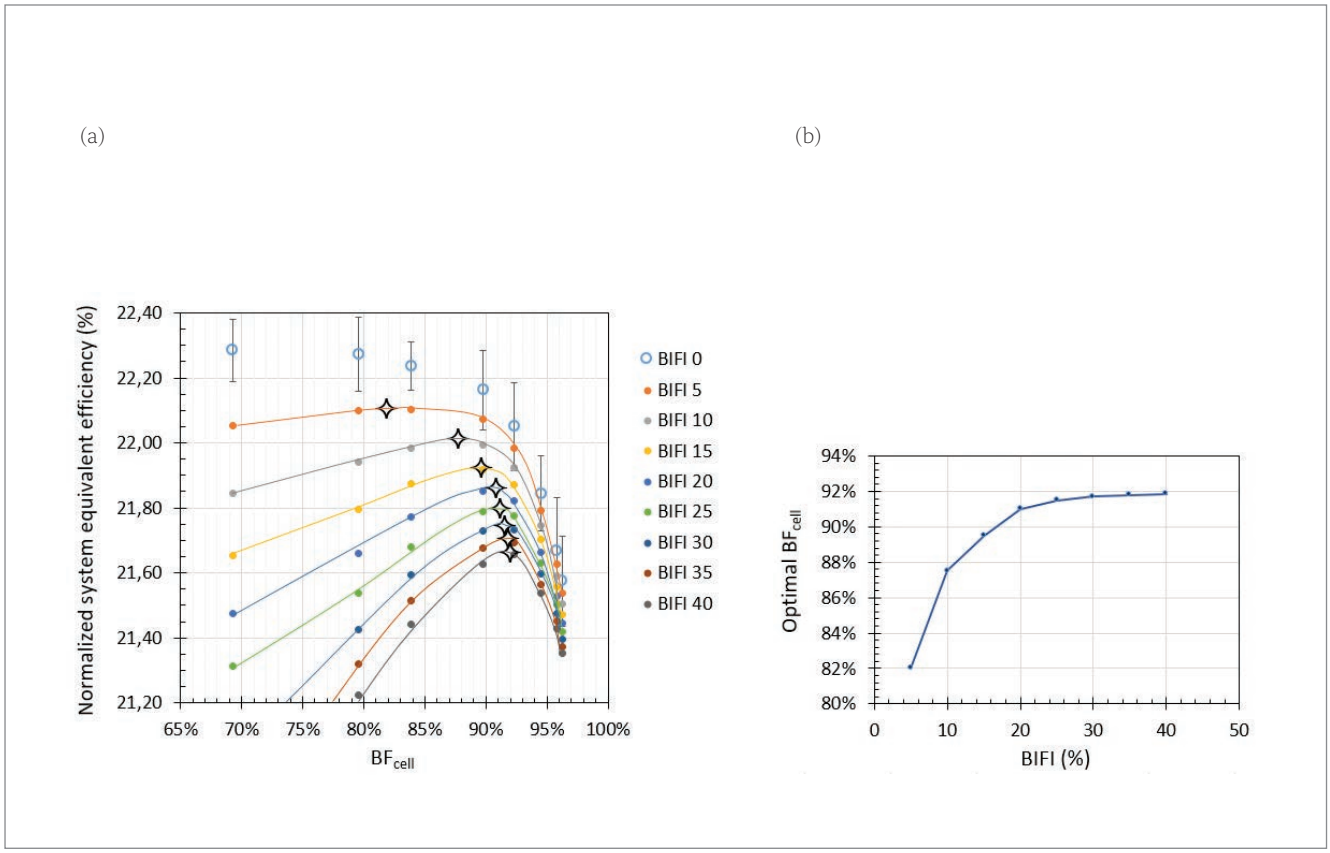


**Figure 7. Cell efficiency without back-side irradiance ($BIFI_{10}$) and estimation of equivalent system efficiency (from the chart in Fig. 6(a)), normalized to the *BIFI* as a function of cell bifaciality. The interpolated lines on graph (a) help to determine the optimal SHJ cell bifaciality, indicated by black stars. This optimal cell bifaciality is plotted against the relative back-side irradiance of the system in graph (b).**

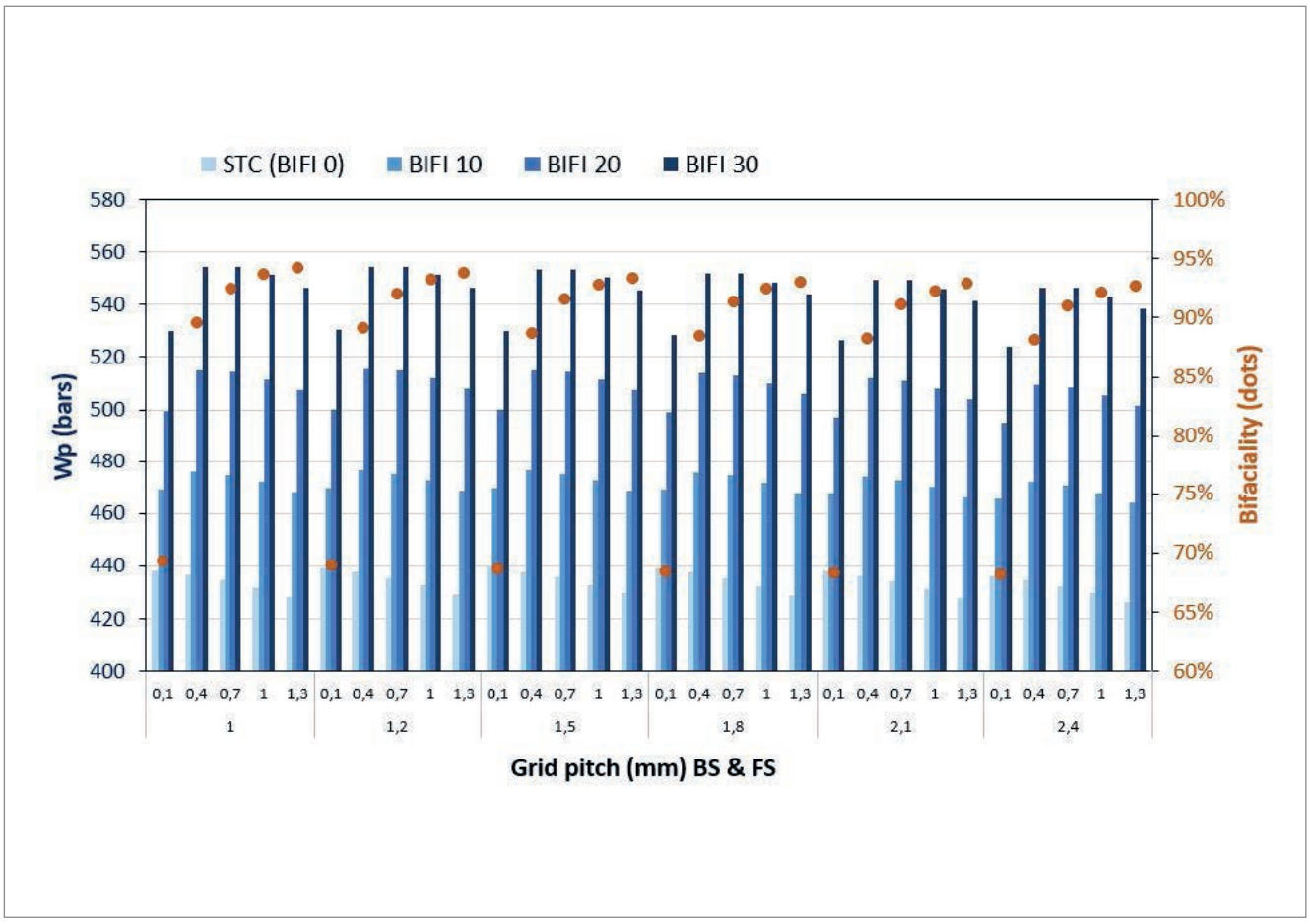


**Figure 8. Simulation data for 144 half-cell (M2) modules with six-busbar prints and various finger pitches (45µm-width considered in all cases), with the power output at STC on the front side and additional *BIFI* on the back side (left scale), and module bifaciality (right scale). The reference cells used in this simulation were processed with PECVD and ITO stacks, optimized for an intrinsic bifaciality of 96.3%, and received a 2.1/0.7mm print, giving an average *I–V* performance of $\eta$ = 22.55%, $V_{oc}$ = 739mV, $I_{sc}$ = 9.342A, *FF* = 79.8% and $BF_{cell}$ = 91.2%.**

for $BIFI_5$ to $BIFI_{30}$, with $BF_{cell}$ ranging from 85% to 95%. This typically corresponds to a FS metal grid pitch from 1.2 to 2mm and a BS pitch from 0.4 to 1mm. With the right optimization of both metal grids for cells with given thin layers, a relative energy gain greater than 1% can be achieved.

For V-EW applications, the optimal cell bifaciality is higher, around 95%, and almost constant, independent of *BIFI*. When considering symmetrical printing, the optimal grid pitch is around 1.5mm, and cell bifaciality is mainly driven by amorphous layer asymmetry.

For monofacial systems, the use of bifacial cells can offer benefits thanks to internal reflection in a glass-backsheet module. The optimization of bifacial SHJ cells for monofacial systems was not experimentally explored in this study, but the model developed to fit and simulate bifacial situations could be used for monofacial applications.

Despite silver printing being the key parameter for $BF_{cell}$, it is important to keep in mind that any progress on layer symmetry, mainly a-Si:H stacks (but also TCO to a lesser extent), can give a global system gain, whatever the type or condition of implementation (bifacial tilted, V-EW, variable *BIFI*, planar connections, monofacial).

Last, but not least, the optimal trend of cell bifaciality ($BF_{cell}$) against relative back-side irradiance (*BIFI*) is reinforced when considering the savings in silver paste when moving to high-bifaciality cells [23]. As an example (see Table 1), for cells optimized with 2.1/0.6mm pitch grids, the average total amount of silver is 127mg/cell. Moving to 2.1/0.9mm grids, cell bifaciality increases by about $2\%_{abs}$ and silver consumption per cell is reduced to 86mg – a 26% saving. For V-EW systems, with the use of an optimized 1.5/1.5mm grid design, cell bifaciality goes to 96.1% and silver consumption is cut to 56mg/cell – a 225% saving!

## Acknowledgement

The authors would like to thank the cell and module R&D teams and pilot production lines at CEA-INES for their contributions (and Joni Mitchell for inspiring the title of this article).

## References

[1] ITRPV 2019, "International technology roadmap for photovoltaic (ITRPV): Results 2018", 10th edn (Mar.) [https://itrpv.vdma.org/en/].

[2] Kopecek, R. et al. 2014, "Bifaciality: One small step for technology, one giant leap for kWh cost reduction", *Photovoltaics International*, 26th edn., pp. 32–45.
[3] 2012–2020, *Proc. Bifi PV Workshops*.
[4] Rodriguez-Gallegos, C.D. et al. 2019, "On the grid metallization optimization design for monofacial and bifacial Si-based PV modules for real-world conditions", *IEEE J. Photovolt.*, Vol. 9-1, pp 112–118.
[5] Kopecek, R. & Libal, J., Eds, 2018, *Bifacial Photovoltaics: Technology, Applications and Economics*. IET.
[6] Rodriguez-Gallegos, C.D. et al. 2018, "Monofacial vs bifacial Si-based PV modules: Which one is more cost-effective?", *Solar Energy*, Vol. 176, pp. 412–438.
[7] Haffner, F. et al. 2020, "The Atacama Desert in Chile as a bifacial hotspot: Yield modelling within the ATAMOSTEC project", *PV Tech Power*, Vol. 24.
[8] Willockx, B. et al. 2020, "Technico-economic study of agrivoltaics systems focusing on orchard crops", *Proc. 37th EU PVSEC* (virtual event).
[9] De Wolf, S. et al. 2012, "High-efficiency silicon heterojunction solar cells: A review", *Green*, Vol. 2, pp. 7–24.
[10] Danel, A. et al. 2019, "Bifaciality optimization of silicon heterojunction solar cells", *Proc. 36th EU PVSEC*, Marseille, France, pp. 224–228.
[11] Danel, A. et al. 2017, "Versatile pilot line to support the heterojunction solar cell industrial development: Busbar and busbar-less configurations", *Proc. 33rd EU PVSEC*, Amsterdam, The Netherlands, pp. 447–450.
[12] Colin, H. et al. 2017, "Energy yield field data of heterojunction-smartwire PV modules", *Proc. 33rd EU PVSEC*, Amsterdam, The Netherlands, 5BV.4.25, poster.
[13] Eisenberg N. & Kreinin, L. 2017, "Understanding energy gain in bifacial PV systems", *PV Tech Power*, Vol. 12, pp. 23–26.
[14] Rodriguez-Gallegos, C.D. et al. 2015, "Analysis and performance of dispensed and screen printed front side contacts on cell and module level", *Proc. 31st EU PVSEC*, Hamburg, Germany, pp. 883–990.
[15] Basset, L. et al. 2018, "Series resistance breakdown of silicon heterojunction solar cells produced on CEA-INES pilot line", *Proc. 35th EU PVSEC*, Brussels, Belgium, pp. 721–724.
[16] Eymard, J. et al. 2019, "Influence of SHJ solar cell bifaciality on the performance of monolithic PV modules", *Proc. 36th EU PVSEC*, Marseille, France, 4AV1.40, poster.
[17] Han, C. et al. 2019, "High-mobility hydrogenated fluorine-doped indium oxide film for passivating contacts c-Si solar cells", *ACS Appl. Mater. Interfaces*, Vol. 11, pp. 45586–45595.
[18] Erfurt, D. et al. 2020, "Aiming for an industrially relevant high-performance TCO for silicon heterojunction solar cells", *Proc. 37th EU PVSEC* (virtual event).
[19] Bivour, M. et al. 2014, "Silicon heterojunction rear emitter solar cells: Less restrictions on the optoelectrical properties of front side TCOs", *Sol. Energy Mater. Sol. Cells,* Vol. 122, pp. 120–129.
[20] Schulte-Huxel, H. et al. 2016, "Flip-flop cell interconnection enabled by an extremely high bifacial factor of screen-printed ion implanted n-PERT Si solar cells", *Proc. 32nd EU PVSEC*, Munich, Germany, pp. 407–412.
[21] Augusto, A. et al. 2016, "Series connection front-to-front and back-to-back of silicon heterojunction solar cells", *Proc. 43rd IEEE PVSC*, Portland, Oregon, USA, pp. 2631–2634.
[22] Favre, W. et al. 2019, "Recent results on the deployment of silicon heterojunction production lines at ENEL Green Power: Influence of the busbar quantity", *Proc. 36th EU PVSEC*, Marseille, France, pp. 235–238.
[23] Faes, A. et al. 2018, "Metallization and interconnection for high-efficiency bifacial silicon heterojunction solar cells and modules", *Photovoltaics International,* 41st edn, pp. 65–76.

"For V-EW systems, with the use of an optimized 1.5/1.5mm grid design, cell bifaciality goes to 96.1% and silver consumption is cut to 56mg/cell – a 225% saving!"

## About the Authors

Adrien Danel holds an M.Sc. in physics and a Ph.D. in microelectronics from INP-Grenoble. From 2004 to 2008 he led the metrology and trace analysis activities at CEA-LETI cleanrooms. He joined CEA-INES in 2009 as the process integration leader on the CEA-INES heterojunction pilot line.

Julien Eymard studied optics, microelectronics and sustainable development at Grenoble INP Phelma and the Institute of Political Studies. Since 2017 he has been a Ph.D. student at CEA-INES, working on the modelling of performance losses in SHJ modules.

Vincent Barth received his Ph.D. in 2014 from the Sorbonne University in the field of organic photovoltaics. He joined CEA-INES in 2017 to work on PV module technology with a focus on interconnection.

Mathieu Tomassini studied physics and chemistry at Joseph Fourier University (Grenoble) before joining 44Solar SARL (Nantes) to work on thin-film solar cell deposition, for which he received his Ph.D. from Nantes University in 2013. He then worked in different areas, from crystalline silicon solar cell defect characterization to PVD process metallization evaluation for organic solar cells. In 2018 he joined CEA-INES, where he works as a process research engineer on the PVD – TCO heterojunction pilot line.

Eric Gerritsen studied physics at Twente University (Netherlands) before joining Philips Research Labs (Eindhoven, NL) in 1985 to work on ion implantation, for which he received his Ph.D. from Groningen University in 1990. He then held various positions at Philips (Lighting, Semiconductors) in Germany, The Netherlands and France, before joining CEA-INES in 2008 to work on PV module technology and applications.

Armand Bettinelli received his Ph.D. in 1987 from Strasbourg University. He worked in industry as a technical manager in the field of high and low cofired ceramics, and then in plasma display panels. In 2005 he joined CEA-INES, where he holds a senior expert position in c-Si solar cell metallization and interconnection.

Charles Roux, head of the CEA-INES HJT lab and pilot line, holds a Ph.D. in II-VI semiconductors from Grenoble University. Prior to joining CEA-INES in 2009, he worked at AMAT as a process engineer in PECVD, PVD, and dry etch for semiconductors. In 2007 he contributed to the start-up of thin-film PV turnkey SunFab at T-Solar in Spain.

## Enquiries

CEA, LITEN
Department of Solar Technologies
INES, F-38000 Grenoble, France

Tel: +33 (0)4 79 79 28 03
Email: adrien.danel@cea.fr